UNIVERSITY NAME (IN BLOCK CAPITALS)

Thesis Title

by

Author Name

A thesis submitted in partial fulfillment for the
degree of Doctor of Philosophy

in the

Faculty Name
Department or School Name

March 2018

Declaration of Authorship

I, AUTHOR NAME, declare that this thesis titled, 'THESIS TITLE' and the work presented in it are my own. I confirm that:

- This work was done wholly or mainly while in candidature for a research degree at this University.
- Where any part of this thesis has previously been submitted for a degree or any other qualification at this University or any other institution, this has been clearly stated.
- Where I have consulted the published work of others, this is always clearly attributed.
- Where I have quoted from the work of others, the source is always given. With the exception of such quotations, this thesis is entirely my own work.
- I have acknowledged all main sources of help.
- Where the thesis is based on work done by myself jointly with others, I have made clear exactly what was done by others and what I have contributed myself.

Signed: _____

Date: _____

"Write a funny quote here."

If the quote is taken from someone, their name goes here

UNIVERSITY NAME (IN BLOCK CAPITALS)

Abstract

Faculty Name
Department or School Name

Doctor of Philosophy

by Author Name

The Thesis Abstract is written here (and usually kept to just this page). The page is kept centered vertically so can expand into the blank space above the title too...

Acknowledgements

The acknowledgements and the people to thank go here, don't forget to include your project advisor...

Contents

List of Figures

List of Tables

Abbreviations

LAH **L**ist **A**bbreviations **H**ere

Physical Constants

Speed of Light $c = 2.997\ 924\ 58 \times 10^8\ \mathrm{ms}^{-\mathrm{S}}$ (exact)

Symbols

a	distance	m
P	power	W (Js^{-1})
ω	angular frequency	rads^{-1}

For/Dedicated to/To my...

Chapter 1

Results

Simulations were peformed on system sizes $L = 40, 48, 64, 80, 104, 128$ with the λs taken from zero to one in steps of 0.2 and also 1.5 where λ_x and λ_y had the same magnitude and the same or opposite signs.

1.1 Linear Case

Figure. 1.1 overlays the Binder cumulant evolution for different sizes in the linear ($\lambda_x = \lambda_y = 0$) case which corresponds to the XY model. Figure. 1.2 does the same but plotted with respect to $t/L^2 \log t$ where the collapse is expected. As is clear, this reobtains the result from XX while using Stochastic evolution rather than Monte Carlo and provides confidence in the results for the non-linear cases. The collapse is not perfect: in Figures 1.3 and **??**, which shows the Binder cumulant as a function of the number of realisations for all the system sizes at two different points, shows how far apart the curves are. For the first case, the uncertainties of the points do not all cross, although none are isolated. In the second case, the collapse is weaker and $L = 40$ is consistently isolated, as can be seen from the graph of the collapse. This also occurs for $L = 64$ earlier on in the simulation. For $L = 48$ this could be an underestimation of the error, and there is a slight downward decrease in its value as the number of realisations is increased. Ideally one would perform further simulations to ensure this, but this was not possible in the time constraints of the project.

With those caveats in mind, we may be assured that the result has been obtained, and this is further corroborated by the plots of $\log n_v$, where n_v is the number of vortices, as a function of $\log(t/\log t)$, shown in XX to XX for each system size. For the linear case, it is expected that $\log n_v = -\log(t/\log t)$. This can be explained as follows: using the result

in XX that the distance between vortices R is approximately proportional to $(t/\log t)^{1/2}$, we have that the vortex density is then $1/R^2$, and the number of vortices $n_v \approx L^2/R^2$, and therefore $\log n_v \approx -\log R^2 = -\log(t/\log t)$ up to some additive constants. As the figures show, the gradient wasobtained to good accuracy for all system sizes. Due to the finite size of the system, the approximation breaks down at large times once the majrotiy of the vortices have annihilated, and therefore a time scale must be chosen with which to calculate the gradient. In practice, the time scale maximised but chosen to be prior to the finite size behaviour of the system. Therefore it is sensible not to read the values literally, but take them as indicative of the XY model behaviour for the linear case.

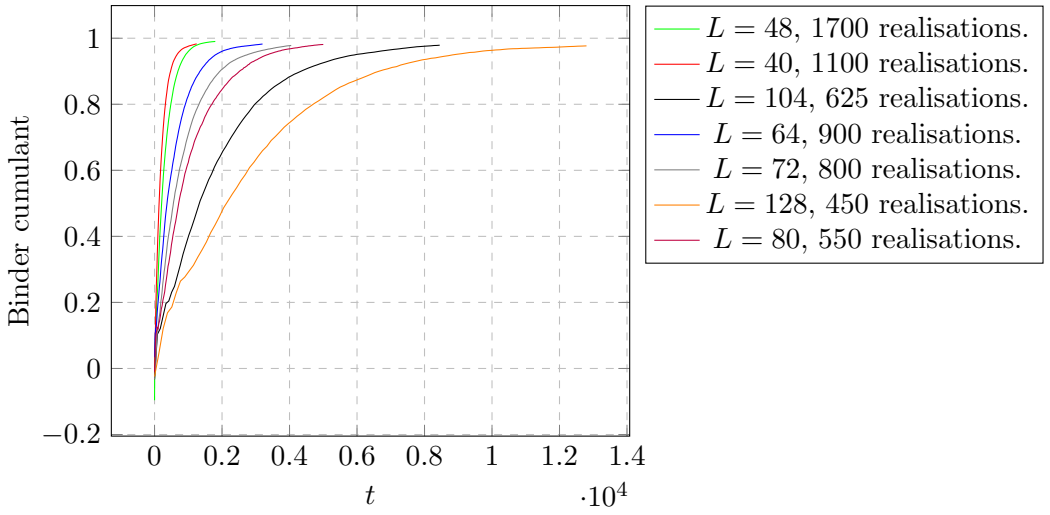

FIGURE 1.1: The Binder cumulant for different sizes with $\lambda_x = \lambda_y = 0$.

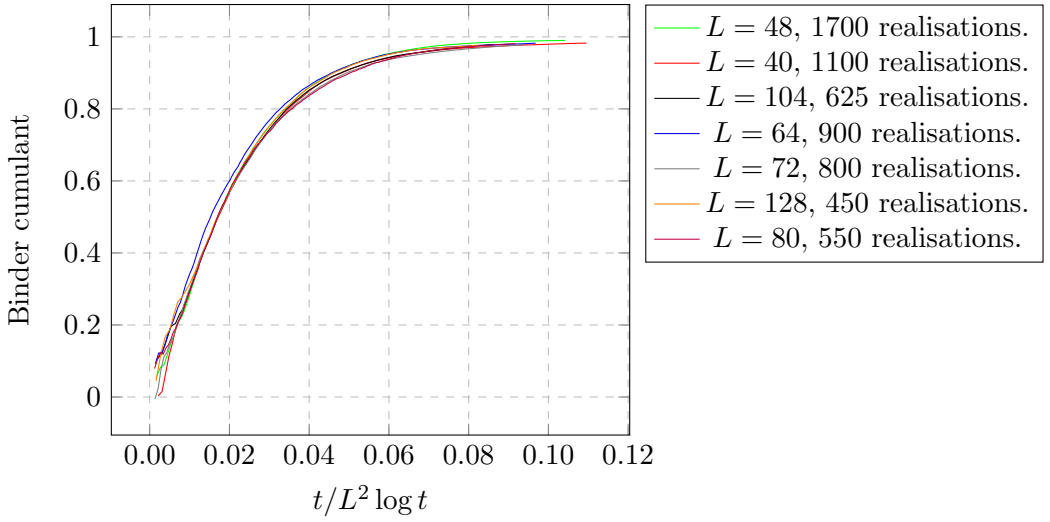

FIGURE 1.2: The Binder cumulant as a function of $t/L^2 \log t$ for different sizes with $\lambda_x = \lambda_y = 0$.

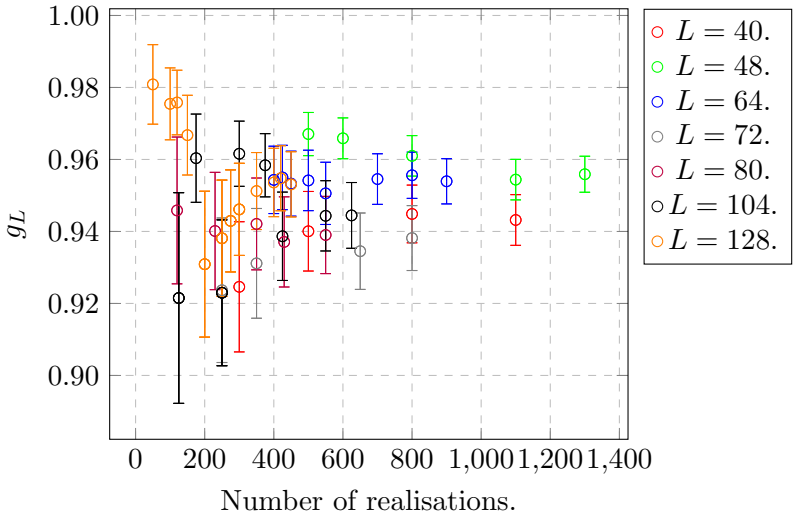

FIGURE 1.3: The uncertainty in the Binder cumulant as a function of the number of realisations at a point closest to $t/L^2 \log t$ for $t = 6500$ (the mid-point of the simulation) for $L = 40.\lambda_x = \lambda_y = 0$.

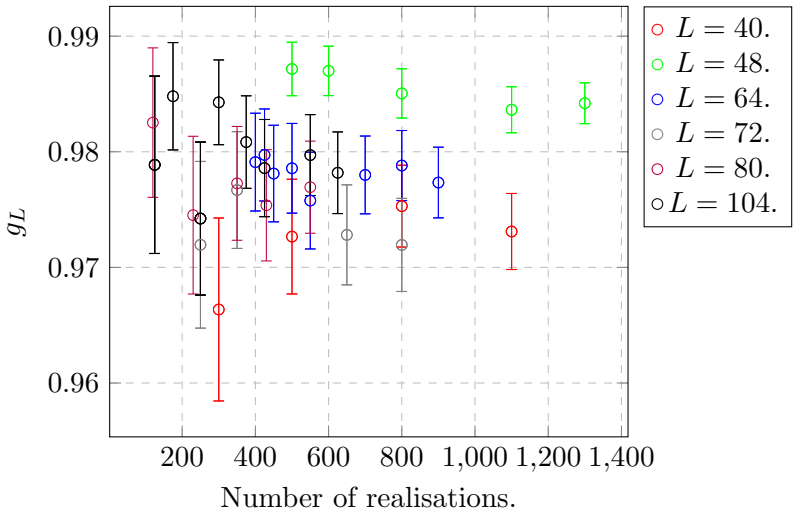

FIGURE 1.4: The uncertainty in the Binder cumulant as a function of the number of realisations at a point closest to $t/L^2 \log t$ for $t = 937.5$ (three quarters through the simualtion) for $L = 40$. $\lambda_x = \lambda_y 0$. There is no value for 128.

1.2 Anistropic Case

For non-zero λs, when $\lambda_x = -\lambda_y$, we expect to obtain the same result as the XY model. Figures **??** to **??** show the Binder cumulant plotted as a function of t and also $t/L^2 \log t$ for several values of increasing λ_x. Although the collapse is not as tight as for the linear case, it clearly still occurs to an extent, confirming the expectation. Due to the errors on the Binder cumulant, which are shown in Figures XX to XX, is not clear whether further realisations are necessary to tighten the collapse further, or if the dynamical exponent growth rate $(t/\log t)^{1/2}$ is simply not as good an approximation as in the linear case. There are clear differences here, however, as the convergence to near one occurs more

rapidly on increasing λ. This is corroborated by fig XX which shows that the gradient in $\log n_v$ where n_v is then number of vortex pairs as a function of $\log(t/\log t)$ decreases on increasing λ, indicating a faster transition to the ordered phase.

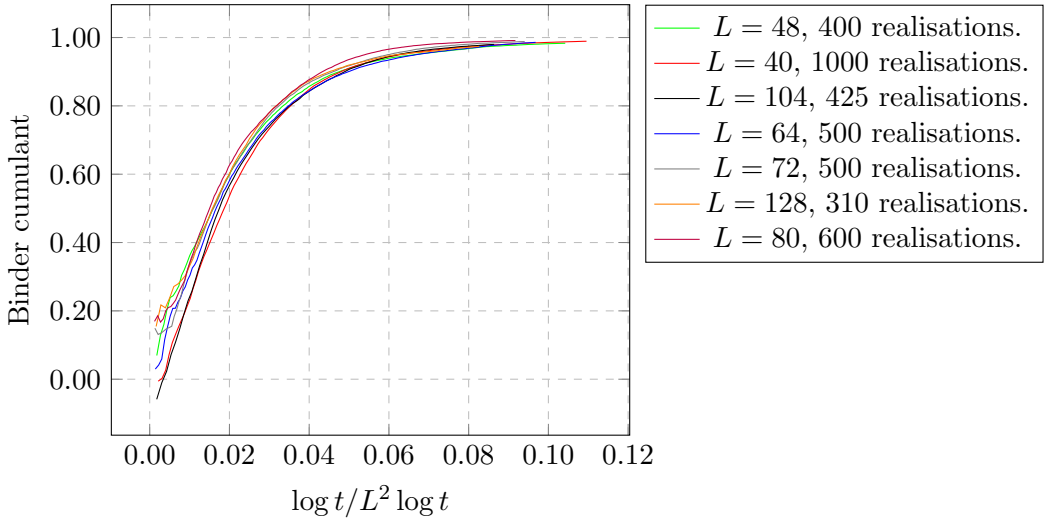

FIGURE 1.5: The Binder cumulant as a function of $t/L^2 \log t$ for different sizes with $\lambda_x = -\lambda_y = 0.2$.

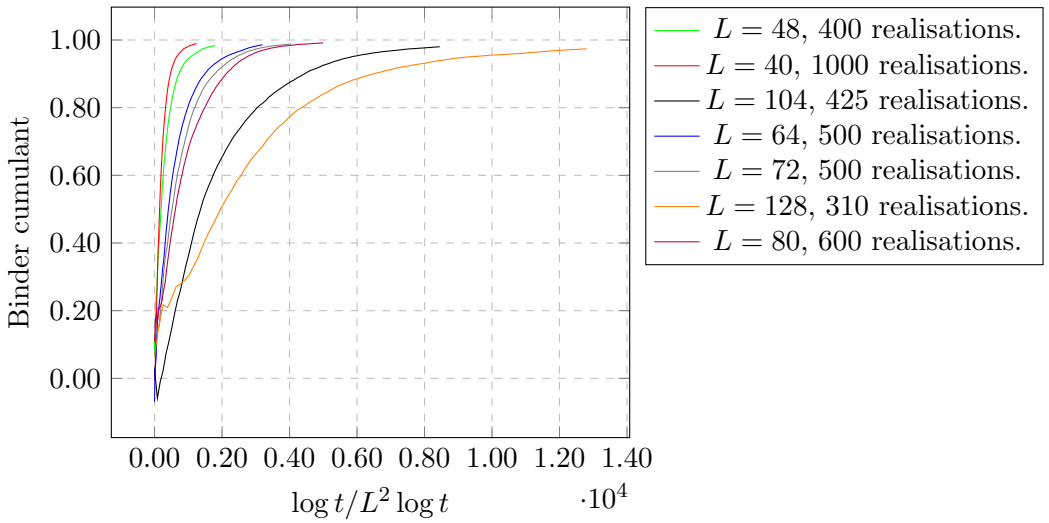

FIGURE 1.6: The Binder cumulant for different sizes with $\lambda_x = -\lambda_y = 0.2$.

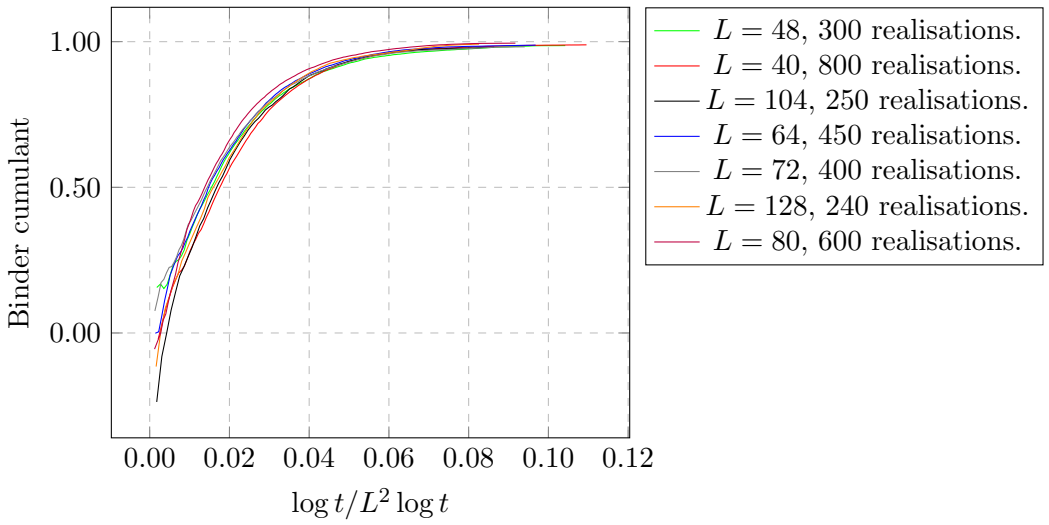

FIGURE 1.7: The Binder cumulant as a function of $t/L^2 \log t$ for different sizes with $\lambda_x = -\lambda_y = 0.4$.

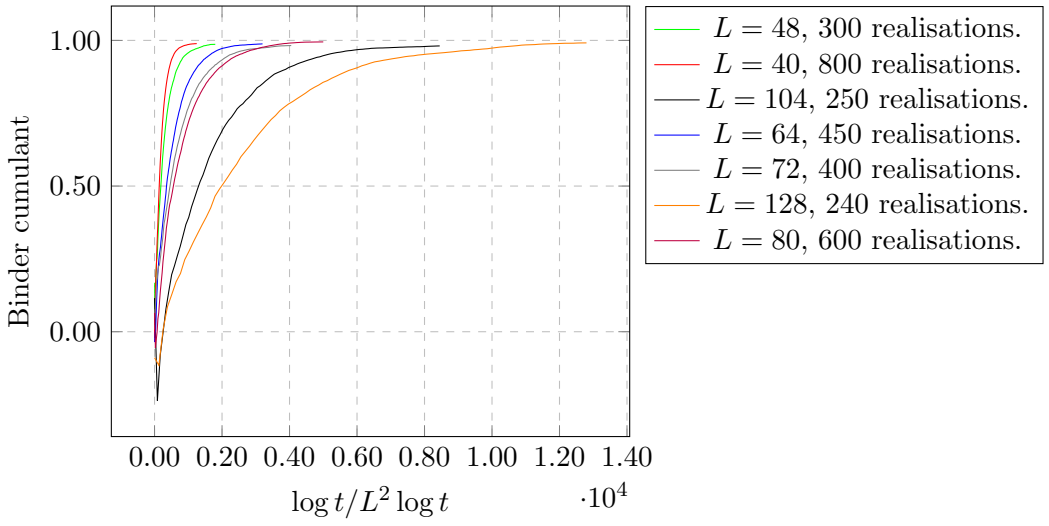

FIGURE 1.8: The Binder cumulant as a function for different sizes with $\lambda_x = -\lambda_y = 0.4$.

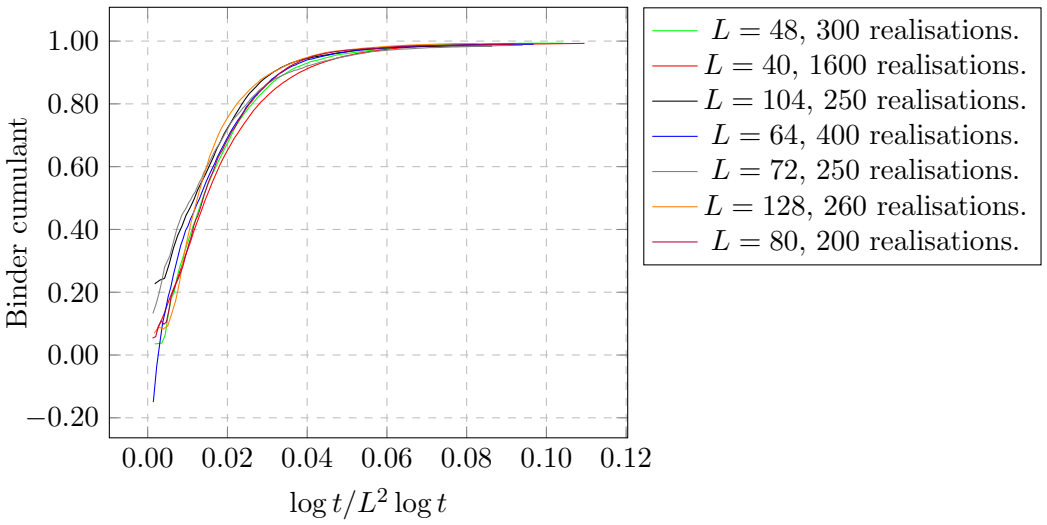

FIGURE 1.9: The Binder cumulant as a function of $t/L^2 \log t$ for different sizes with $\lambda_x = -\lambda_y = 0.6$.

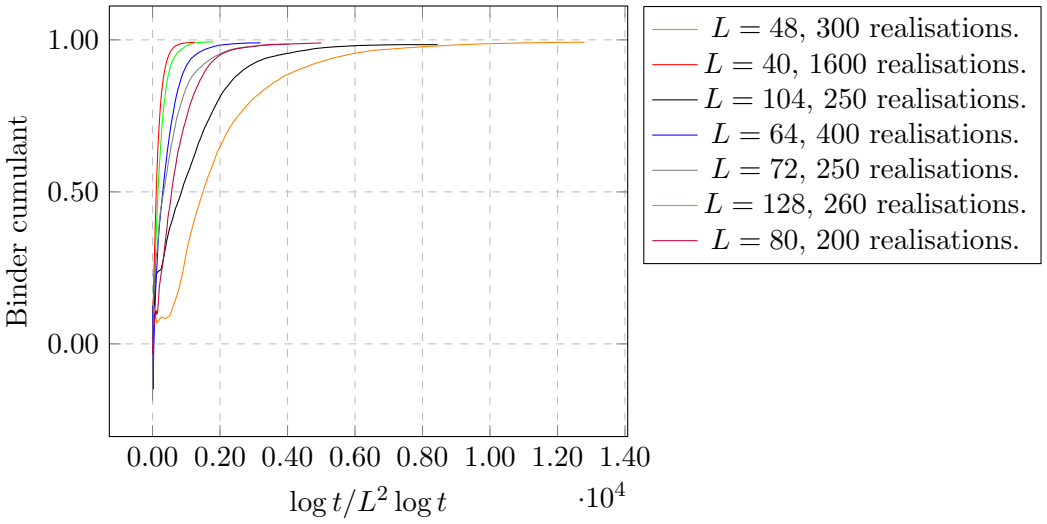

FIGURE 1.10: The Binder cumulant for different sizes with $\lambda_x = -\lambda_y = 0.6$.

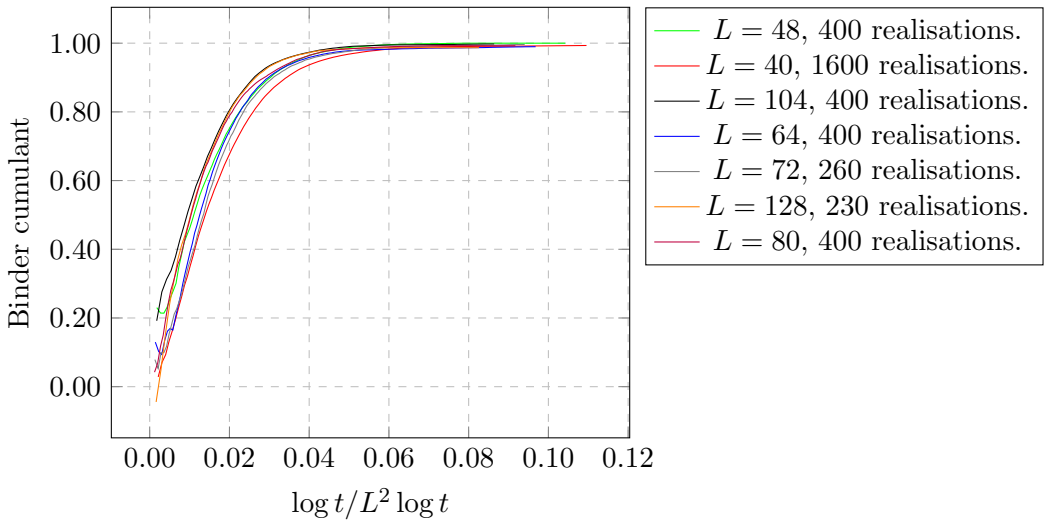

FIGURE 1.11: The Binder cumulant as a function of $t/L^2 \log t$ for different sizes with $\lambda_x = -\lambda_y = 0.8$.

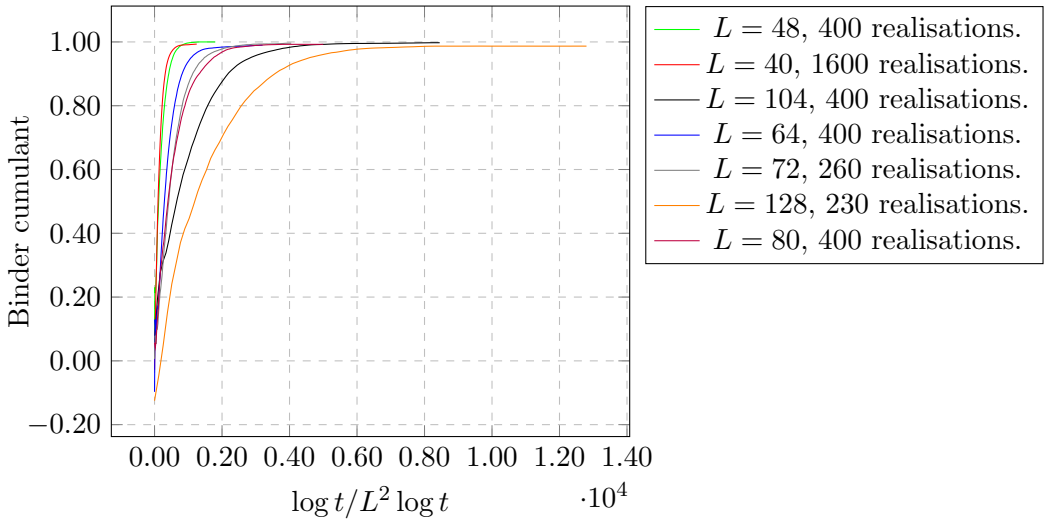

FIGURE 1.12: The Binder cumulant for different sizes with $\lambda_x = -\lambda_y = 0.8$.

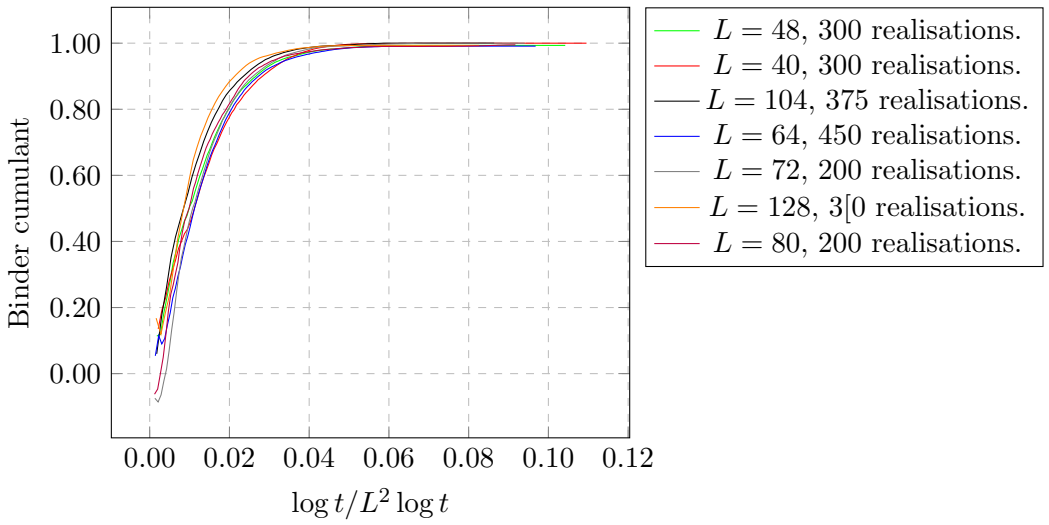

FIGURE 1.13: The Binder cumulant as a function of $t/L^2 \log t$ for different sizes with $\lambda_x = -\lambda_y = 1$.

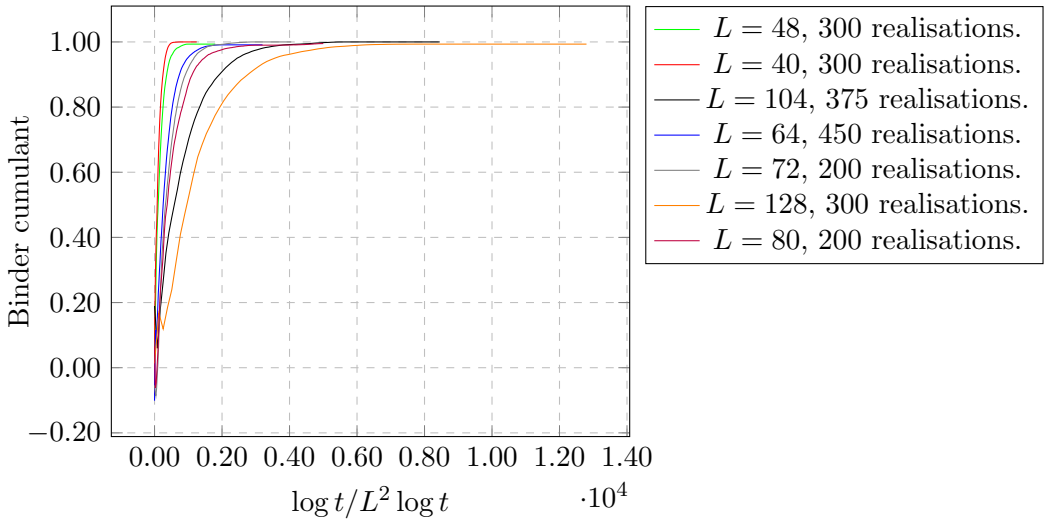

FIGURE 1.14: The Binder cumulant for different sizes with $\lambda_x = -\lambda_y = 1$.

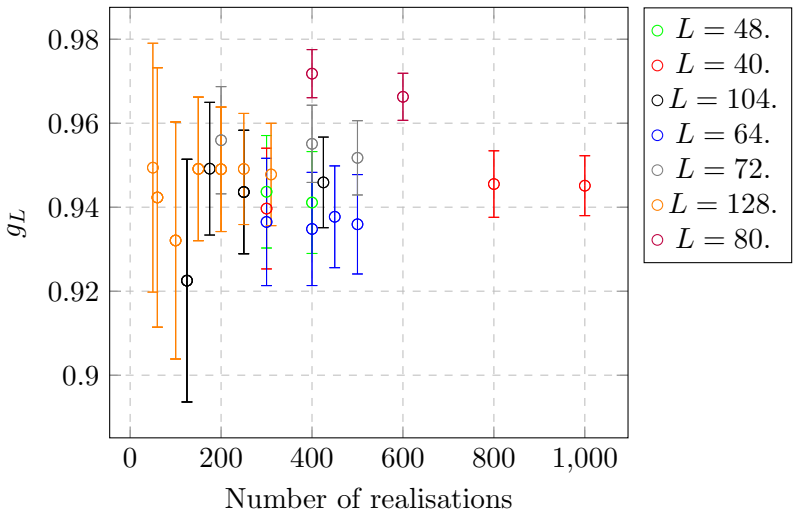

FIGURE 1.15: The uncertainty in the Binder cumulant as a function of the number of realisations at a point closest to $t/L^2 \log t$ for $t = 6500$ (the mid-point of the simulation) for $L = 40.\lambda_x = -\lambda_y = 0.2$.

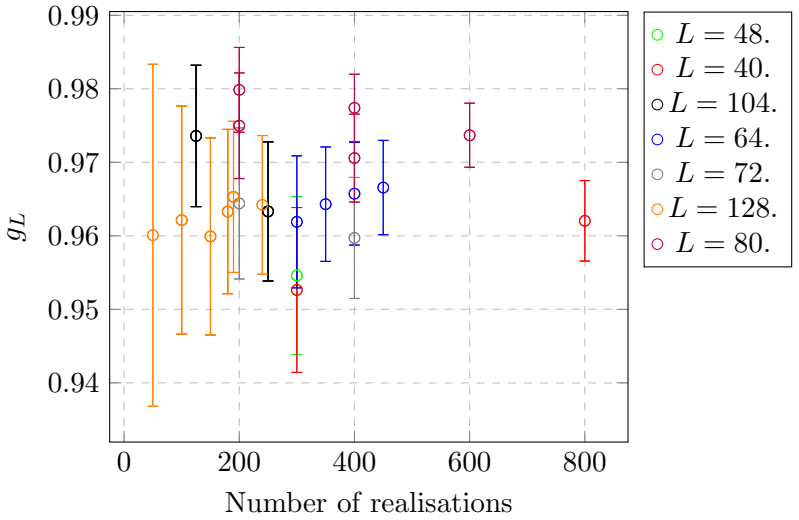

FIGURE 1.16: The uncertainty in the Binder cumulant as a function of the number of realisations at a point closest to $t/L^2 \log t$ for $t = 6500$ (the mid-point of the simulation) for $L = 40.\lambda_x = -\lambda_y = 0.4$.

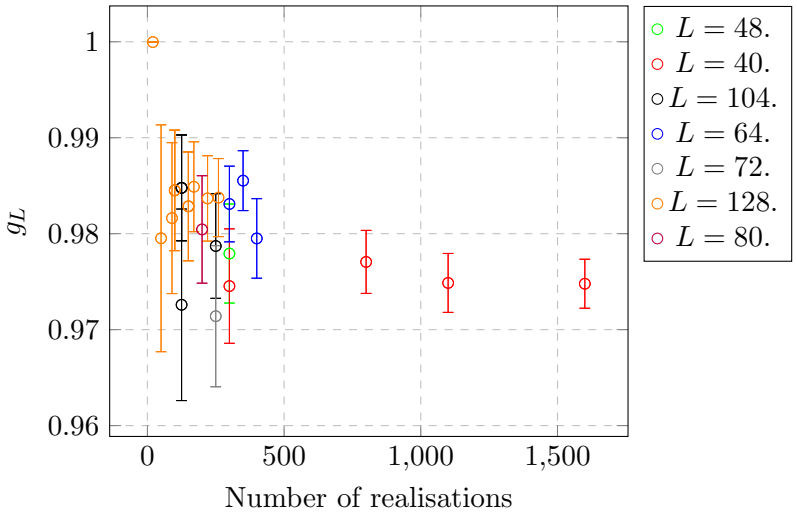

FIGURE 1.17: The uncertainty in the Binder cumulant as a function of the number of realisations at a point closest to $t/L^2 \log t$ for $t = 6500$ (the mid-point of the simulation) for $L = 40.\lambda_x = -\lambda_y = 0.6$.

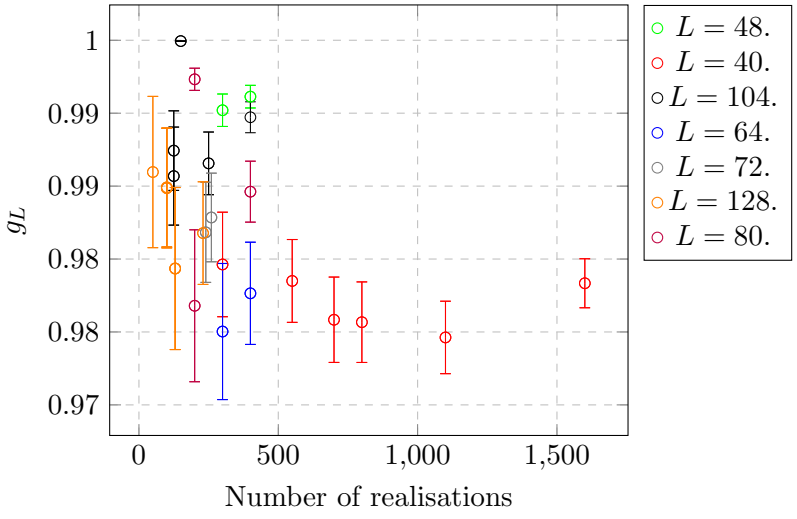

FIGURE 1.18: The uncertainty in the Binder cumulant as a function of the number of realisations at a point closest to $t/L^2 \log t$ for $t = 6500$ (the mid-point of the simulation) for $L = 40.\lambda_x = -\lambda_y = 0.8$.

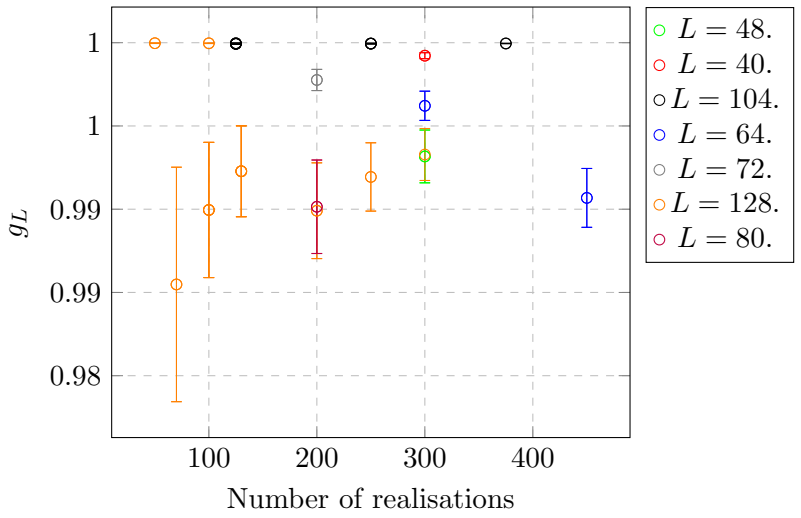

FIGURE 1.19: The uncertainty in the Binder cumulant as a function of the number of realisations at a point closest to $t/L^2 \log t$ for $t = 6500$ (the mid-point of the simulation) for $L = 40$. $\lambda_x = -\lambda_y = 1$.

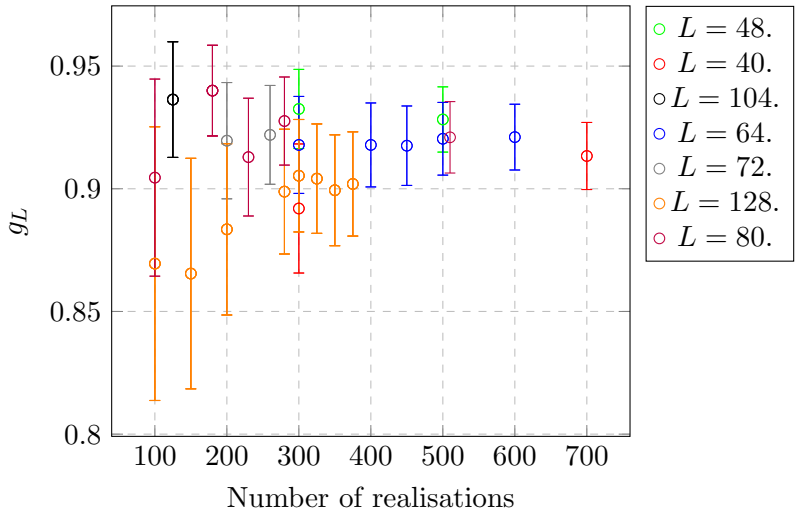

FIGURE 1.20: The uncertainty in the Binder cumulant as a function of the number of realisations at a point closest to $t/L^2 \log t$ for $t = 6500$ (the mid-point of the simulation) for $L = 40.\lambda_x = \lambda_y = 0.2$.

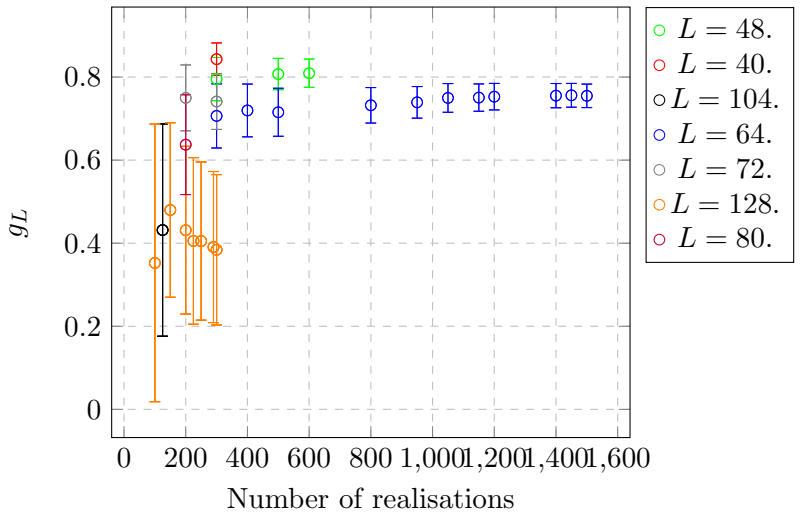

FIGURE 1.21: The uncertainty in the Binder cumulant as a function of the number of realisations at a point closest to $t/L^2 \log t$ for $t = 6500$ (the mid-point of the simulation) for $L = 40.\lambda_x = \lambda_y = 0.4$.

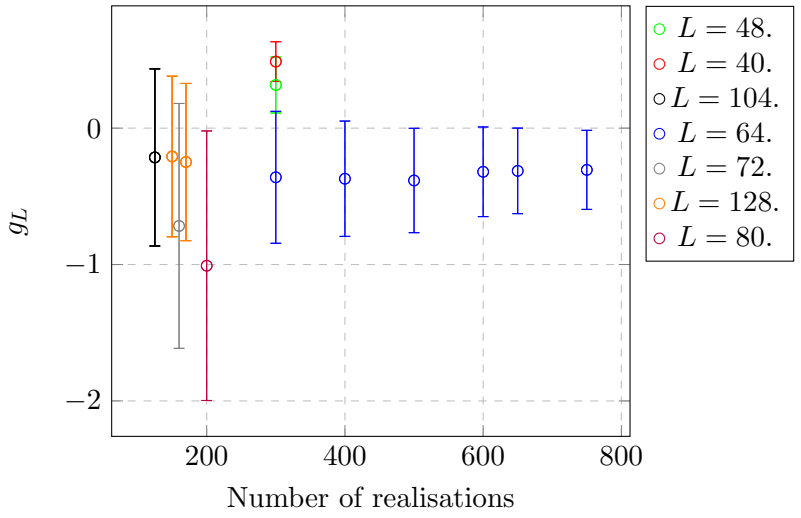

FIGURE 1.22: The uncertainty in the Binder cumulant as a function of the number of realisations at a point closest to $t/L^2 \log t$ for $t = 6500$ (the mid-point of the simulation) for $L = 40.\lambda_x = \lambda_y = 0.6$.

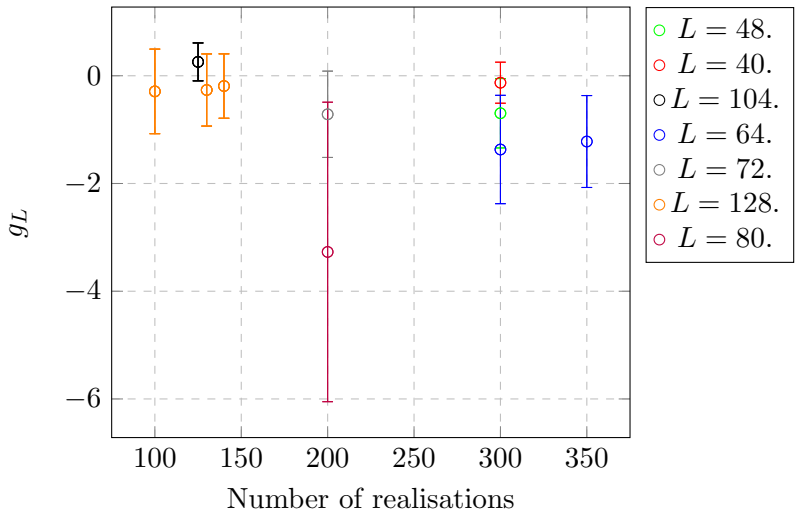

FIGURE 1.23: The uncertainty in the Binder cumulant as a function of the number of realisations at a point closest to $t/L^2 \log t$ for $t = 6500$ (the mid-point of the simulation) for $L = 40.\lambda_x = \lambda_y = 0.8$.

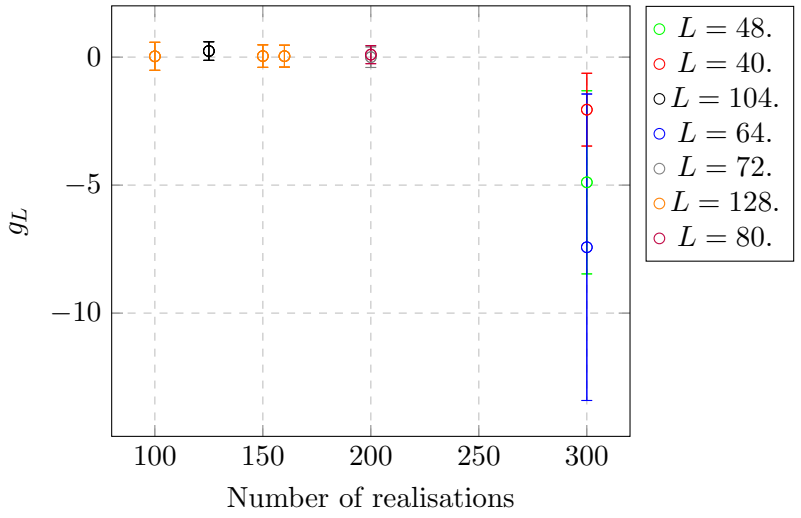

FIGURE 1.24: The uncertainty in the Binder cumulant as a function of the number of realisations at a point closest to $t/L^2 \log t$ for $t = 6500$ (the mid-point of the simulation) for $L = 40.\lambda_x = \lambda_y = 1$.

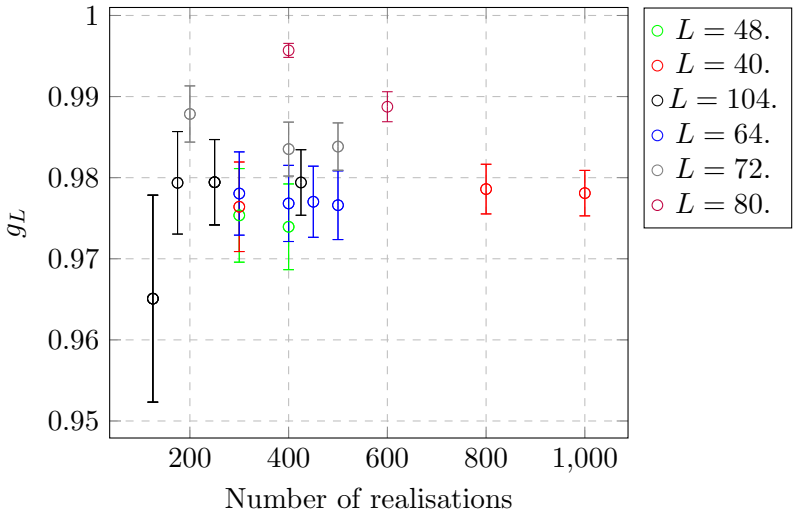

FIGURE 1.25: The uncertainty in the Binder cumulant as a function of the number of realisations at a point closest to $t/L^2 \log t$ for $t = 937.5$ (three quarters through the simualtion) for $L = 40$. $\lambda_x = -\lambda_y = 0.2$. There is no value for 128.

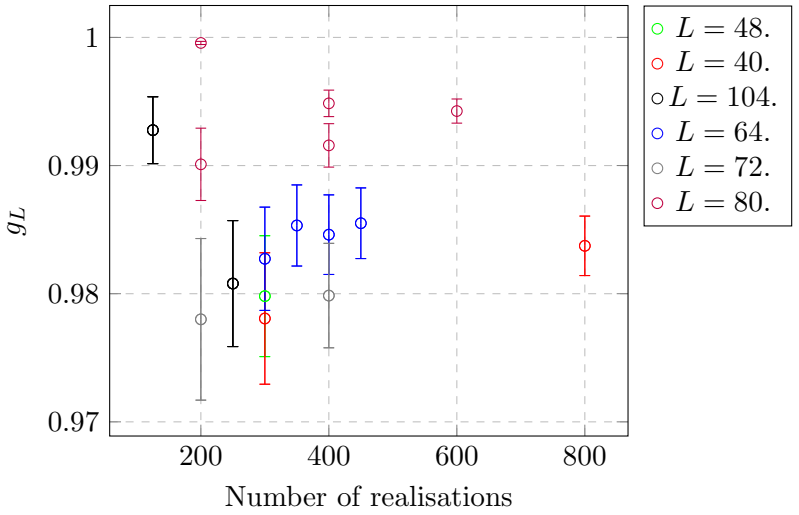

FIGURE 1.26: The uncertainty in the Binder cumulant as a function of the number of realisations at a point closest to $t/L^2 \log t$ for $t = 937.5$ (three quarters through the simualtion) for $L = 40$. $\lambda_x = \lambda_y - 0.4$ There is no value for 128.

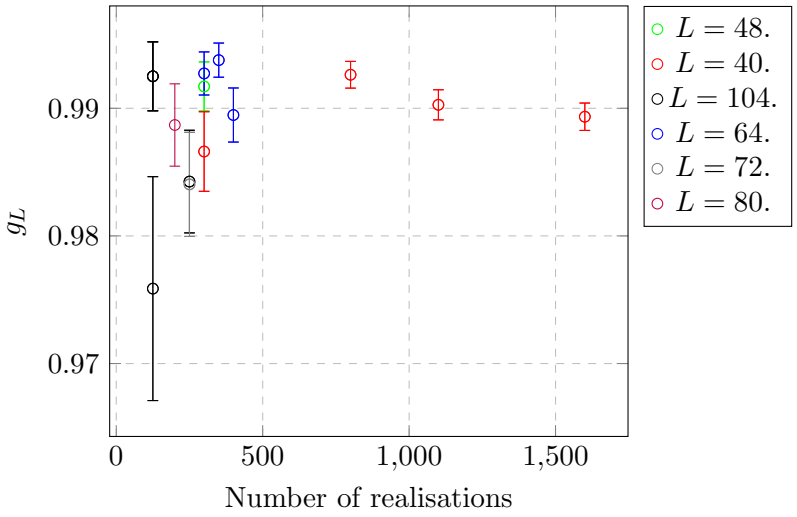

FIGURE 1.27: The uncertainty in the Binder cumulant as a function of the number of realisations at a point closest to $t/L^2 \log t$ for $t = 937.5$ (three quarters through the simualtion) for $L = 40$. $\lambda_x = -\lambda_y = 0.6$ There is no value for 128.

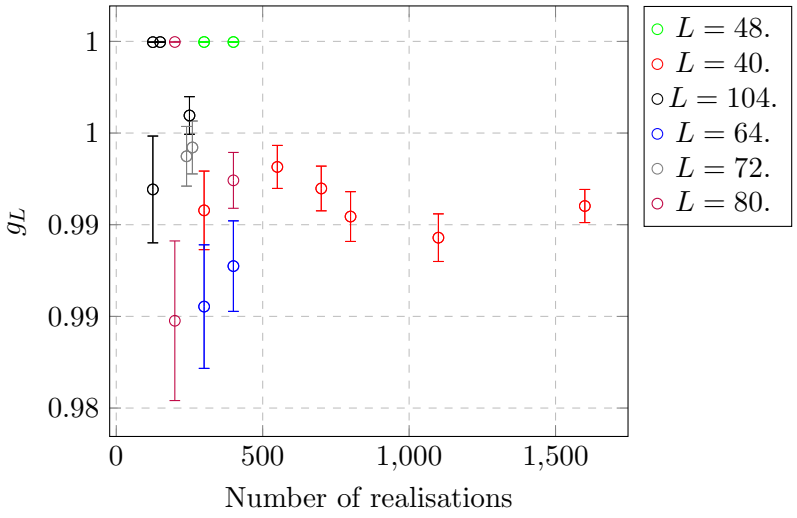

FIGURE 1.28: The uncertainty in the Binder cumulant as a function of the number of realisations at a point closest to $t/L^2 \log t$ for $t = 937.5$ (three quarters through the simualtion) for $L = 40$. $\lambda_x = -\lambda_y = 0.8$. There is no value for 128.

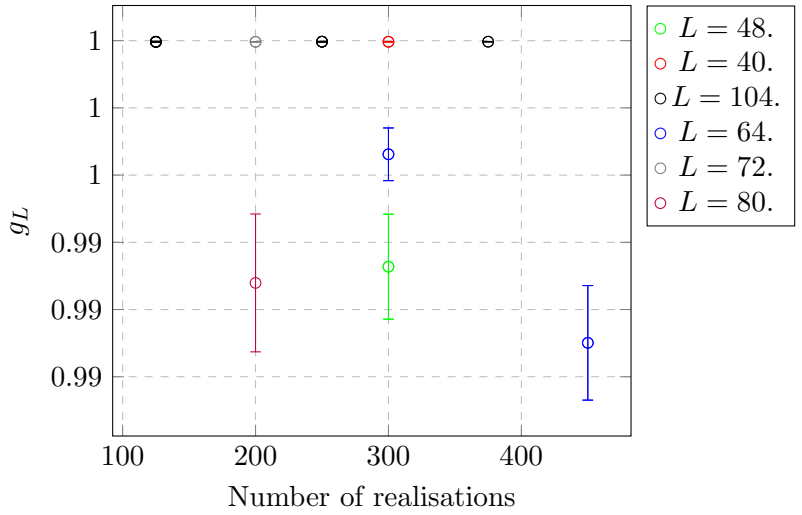

FIGURE 1.29: The uncertainty in the Binder cumulant as a function of the number of realisations at a point closest to $t/L^2 \log t$ for $t = 937.5$ (three quarters through the simualtion) for $L = 40$. $\lambda_x = -\lambda_y = 1$. There is no value for 128.

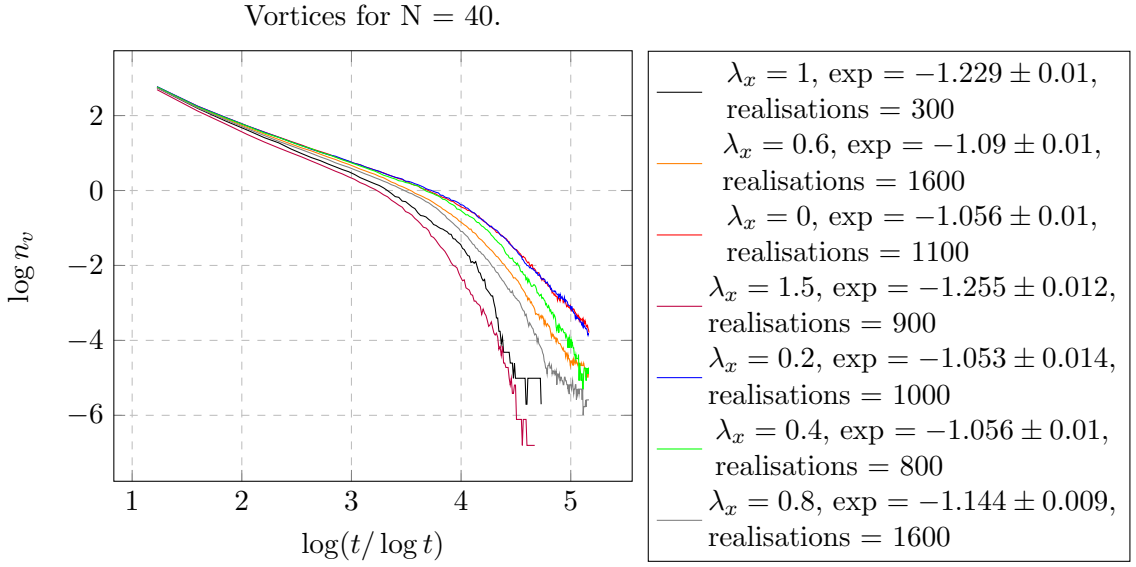

Vortices for N = 48.

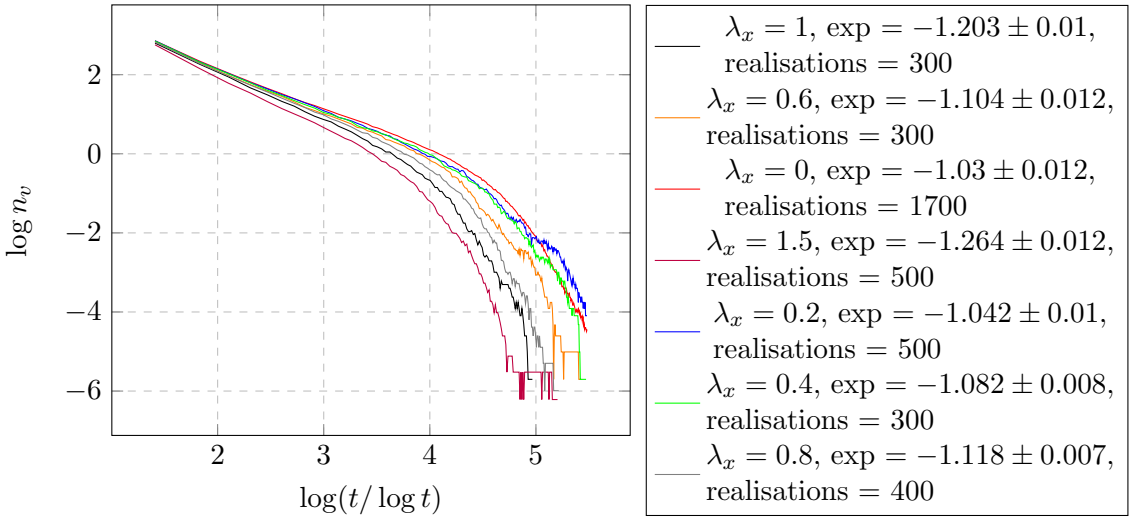

Vortices for N = 64.

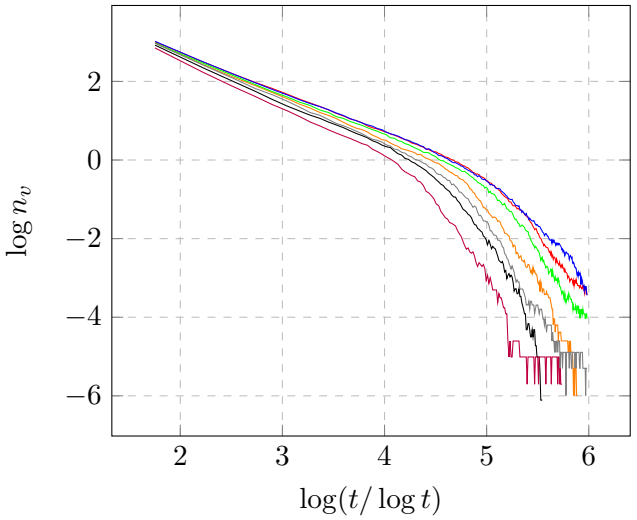

$\lambda_x = 1$, exp $= -1.095 \pm 0.009$, realisations $= 450$
$\lambda_x = 0.6$, exp $= -1.083 \pm 0.008$, realisations $= 400$
$\lambda_x = 0$, exp $= -0.999 \pm 0.004$, realisations $= 900$
$\lambda_x = 1.5$, exp $= -1.165 \pm 0.008$, realisations $= 300$
$\lambda_x = 0.2$, exp $= -0.98 \pm 0.005$, realisations $= 500$
$\lambda_x = 0.4$, exp $= -1.007 \pm 0.006$, realisations $= 450$
$\lambda_x = 0.8$, exp $= -1.123 \pm 0.006$, realisations $= 400$

Vortices for N = 128.

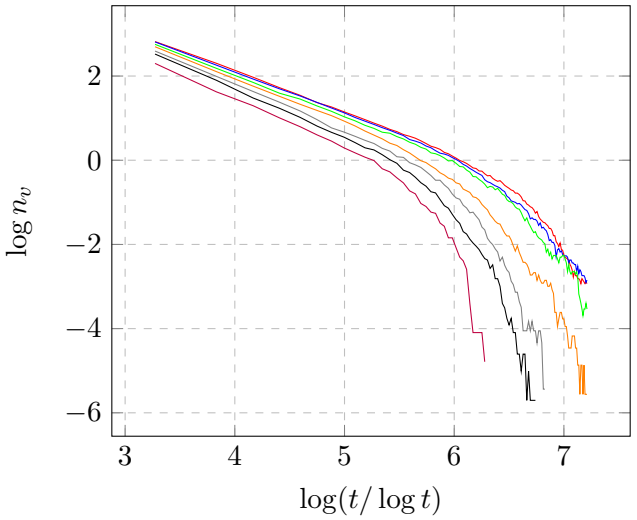

$\lambda_x = 1$, exp $= -1.162 \pm 0.016$, realisations $= 300$
$\lambda_x = 0.6$, exp $= -1.001 \pm 0.007$, realisations $= 260$
$\lambda_x = 0$, exp $= -0.995 \pm 0.01$, realisations $= 450$
$\lambda_x = 1.5$, exp $= -1.146 \pm 0.023$, realisations $= 120$
$\lambda_x = 0.2$, exp $= -0.968 \pm 0.005$, realisations $= 310$
$\lambda_x = 0.4$, exp $= -0.974 \pm 0.015$, realisations $= 240$
$\lambda_x = 0.8$, exp $= -1.153 \pm 0.028$, realisations $= 230$

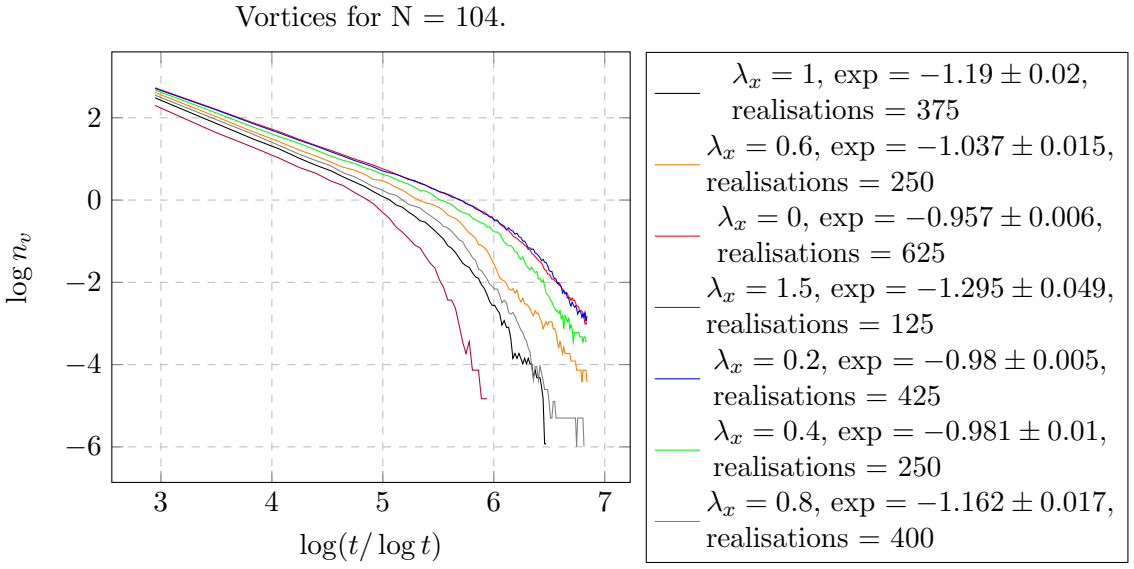
Vortices for N = 104.
log n_v
2
0
−2
−4
−6
3
4
5
6
7
log(t/ log t)
$\lambda_x = 1$, exp = -1.19 ± 0.02, realisations = 375
$\lambda_x = 0.6$, exp = -1.037 ± 0.015, realisations = 250
$\lambda_x = 0$, exp = -0.957 ± 0.006, realisations = 625
$\lambda_x = 1.5$, exp = -1.295 ± 0.049, realisations = 125
$\lambda_x = 0.2$, exp = -0.98 ± 0.005, realisations = 425
$\lambda_x = 0.4$, exp = -0.981 ± 0.01, realisations = 250
$\lambda_x = 0.8$, exp = -1.162 ± 0.017, realisations = 400

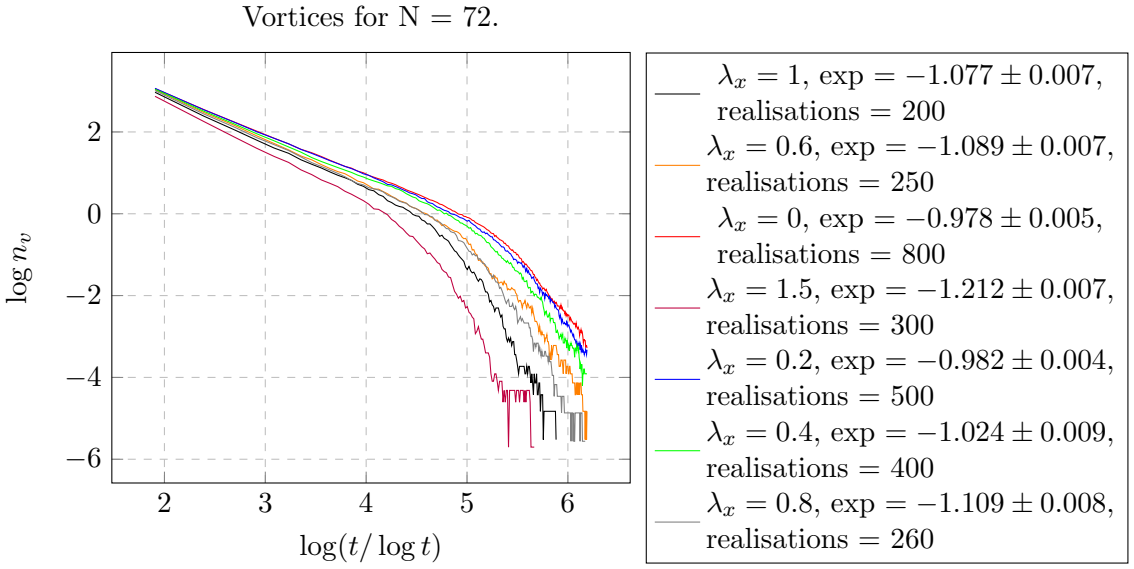
Vortices for N = 72.
log n_v
2
0
−2
−4
−6
2
3
4
5
6
log(t/ log t)
$\lambda_x = 1$, exp $= -1.077 \pm 0.007$, realisations $= 200$
$\lambda_x = 0.6$, exp $= -1.089 \pm 0.007$, realisations $= 250$
$\lambda_x = 0$, exp $= -0.978 \pm 0.005$, realisations $= 800$
$\lambda_x = 1.5$, exp $= -1.212 \pm 0.007$, realisations $= 300$
$\lambda_x = 0.2$, exp $= -0.982 \pm 0.004$, realisations $= 500$
$\lambda_x = 0.4$, exp $= -1.024 \pm 0.009$, realisations $= 400$
$\lambda_x = 0.8$, exp $= -1.109 \pm 0.008$, realisations $= 260$

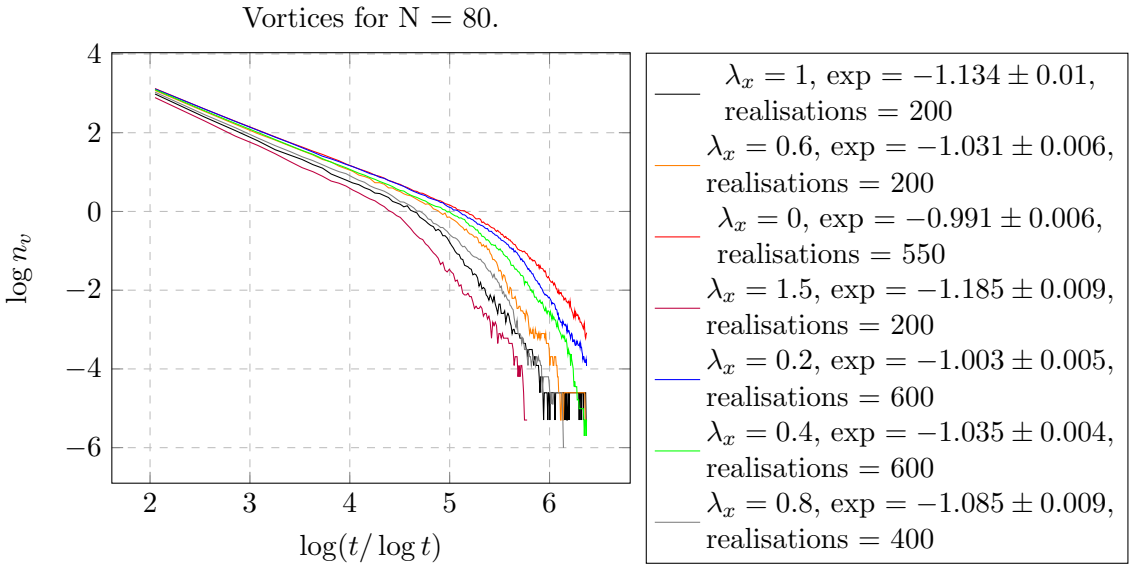
Vortices for N = 80.
log n_v
4
2
0
−2
−4
−6
2
3
4
5
6
log(t/ log t)
$\lambda_x = 1$, exp $= -1.134 \pm 0.01$, realisations $= 200$
$\lambda_x = 0.6$, exp $= -1.031 \pm 0.006$, realisations $= 200$
$\lambda_x = 0$, exp $= -0.991 \pm 0.006$, realisations $= 550$
$\lambda_x = 1.5$, exp $= -1.185 \pm 0.009$, realisations $= 200$
$\lambda_x = 0.2$, exp $= -1.003 \pm 0.005$, realisations $= 600$
$\lambda_x = 0.4$, exp $= -1.035 \pm 0.004$, realisations $= 600$
$\lambda_x = 0.8$, exp $= -1.085 \pm 0.009$, realisations $= 400$

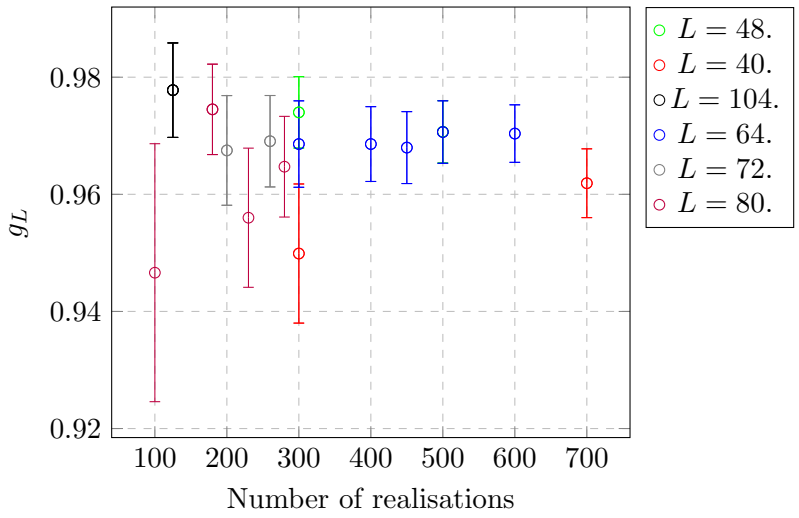

FIGURE 1.30: The uncertainty in the Binder cumulant as a function of the number of realisations at a point closest to $t/L^2 \log t$ for $t = 937.5$ (three quarters through the simualtion) for $L = 40$. $\lambda_x = \lambda_y = 0.2$. There is no value for 128.

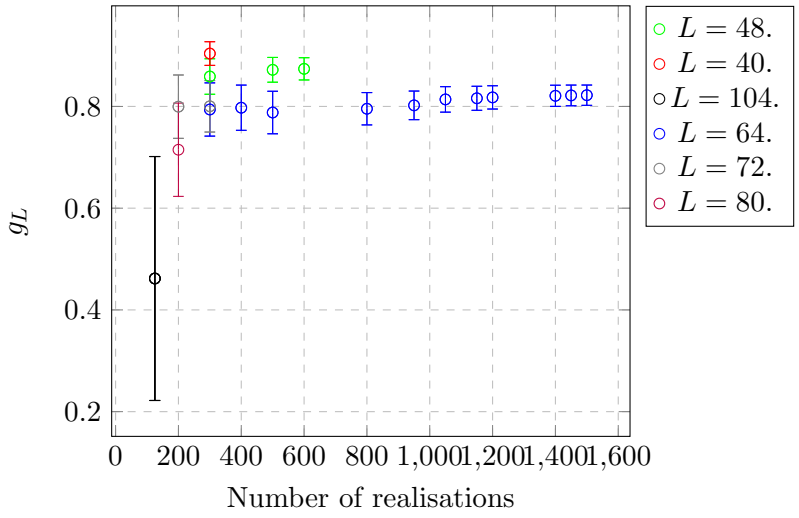

FIGURE 1.31: The uncertainty in the Binder cumulant as a function of the number of realisations at a point closest to $t/L^2 \log t$ for $t = 937.5$ (three quarters through the simualtion) for $L = 40$. $\lambda_x = \lambda_y = 0.4$. There is no value for 128.

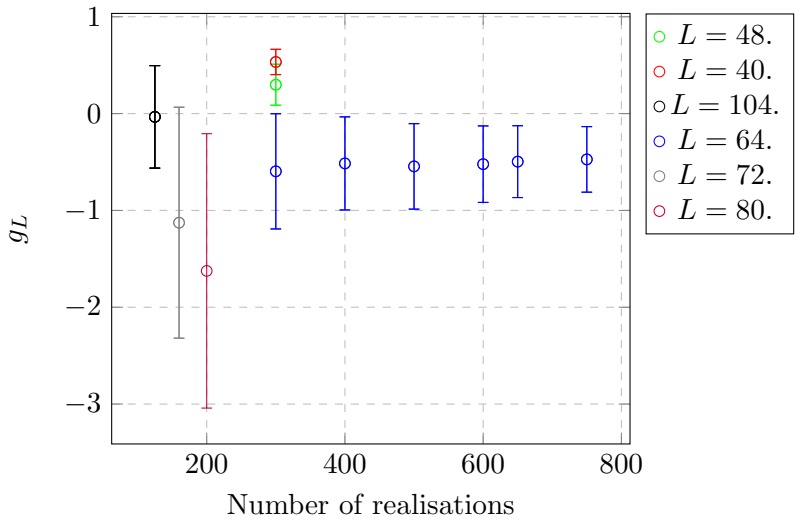

FIGURE 1.32: The uncertainty in the Binder cumulant as a function of the number of realisations at a point closest to $t/L^2 \log t$ for $t = 937.5$ (three quarters through the simualtion) for $L = 40$. $\lambda_x = \lambda_y = 0.6$. There is no value for 128.

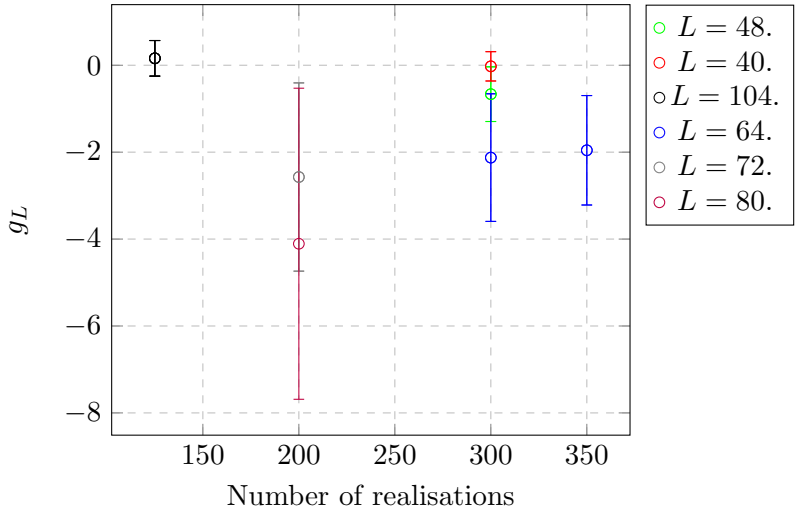

FIGURE 1.33: The uncertainty in the Binder cumulant as a function of the number of realisations at a point closest to $t/L^2 \log t$ for $t = 937.5$ (three quarters through the simualtion) for $L = 40$. $\lambda_x = \lambda_y = 0.8$. There is no value for 128.

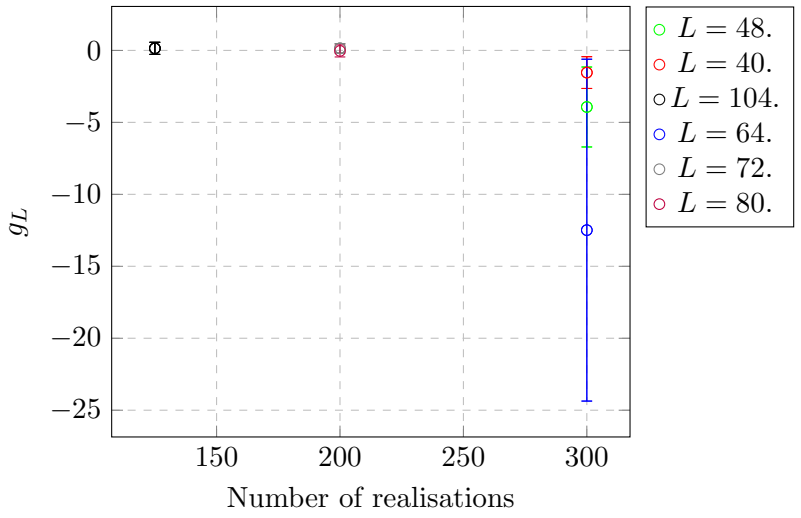

FIGURE 1.34: The uncertainty in the Binder cumulant as a function of the number of realisations at a point closest to $t/L^2 \log t$ for $t = 937.5$ (three quarters through the simualtion) for $L = 40$. $\lambda_x = \lambda_y = 1$. There is no value for 128.

Appendix A

An Appendix

Lorem ipsum dolor sit amet, consectetur adipiscing elit. Vivamus at pulvinar nisi. Phasellus hendrerit, diam placerat interdum iaculis, mauris justo cursus risus, in viverra purus eros at ligula. Ut metus justo, consequat a tristique posuere, laoreet nec nibh. Etiam et scelerisque mauris. Phasellus vel massa magna. Ut non neque id tortor pharetra bibendum vitae sit amet nisi. Duis nec quam quam, sed euismod justo. Pellentesque eu tellus vitae ante tempus malesuada. Nunc accumsan, quam in congue consequat, lectus lectus dapibus erat, id aliquet urna neque at massa. Nulla facilisi. Morbi ullamcorper eleifend posuere. Donec libero leo, faucibus nec bibendum at, mattis et urna. Proin consectetur, nunc ut imperdiet lobortis, magna neque tincidunt lectus, id iaculis nisi justo id nibh. Pellentesque vel sem in erat vulputate faucibus molestie ut lorem.

Quisque tristique urna in lorem laoreet at laoreet quam congue. Donec dolor turpis, blandit non imperdiet aliquet, blandit et felis. In lorem nisi, pretium sit amet vestibulum sed, tempus et sem. Proin non ante turpis. Nulla imperdiet fringilla convallis. Vivamus vel bibendum nisl. Pellentesque justo lectus, molestie vel luctus sed, lobortis in libero. Nulla facilisi. Aliquam erat volutpat. Suspendisse vitae nunc nunc. Sed aliquet est suscipit sapien rhoncus non adipiscing nibh consequat. Aliquam metus urna, faucibus eu vulputate non, luctus eu justo.

Donec urna leo, vulputate vitae porta eu, vehicula blandit libero. Phasellus eget massa et leo condimentum mollis. Nullam molestie, justo at pellentesque vulputate, sapien velit ornare diam, nec gravida lacus augue non diam. Integer mattis lacus id libero ultrices sit amet mollis neque molestie. Integer ut leo eget mi volutpat congue. Vivamus sodales, turpis id venenatis placerat, tellus purus adipiscing magna, eu aliquam nibh dolor id nibh. Pellentesque habitant morbi tristique senectus et netus et malesuada fames ac turpis egestas. Sed cursus convallis quam nec vehicula. Sed vulputate neque eget odio fringilla ac sodales urna feugiat.

Phasellus nisi quam, volutpat non ullamcorper eget, congue fringilla leo. Cras et erat et nibh placerat commodo id ornare est. Nulla facilisi. Aenean pulvinar scelerisque eros eget interdum. Nunc pulvinar magna ut felis varius in hendrerit dolor accumsan. Nunc pellentesque magna quis magna bibendum non laoreet erat tincidunt. Nulla facilisi.

Duis eget massa sem, gravida interdum ipsum. Nulla nunc nisl, hendrerit sit amet commodo vel, varius id tellus. Lorem ipsum dolor sit amet, consectetur adipiscing elit. Nunc ac dolor est. Suspendisse ultrices tincidunt metus eget accumsan. Nullam facilisis, justo vitae convallis sollicitudin, eros augue malesuada metus, nec sagittis diam nibh ut sapien. Duis blandit lectus vitae lorem aliquam nec euismod nisi volutpat. Vestibulum ornare dictum tortor, at faucibus justo tempor non. Nulla facilisi. Cras non massa nunc, eget euismod purus. Nunc metus ipsum, euismod a consectetur vel, hendrerit nec nunc.